Epigenetic reversion of breast carcinoma phenotype is accompanied by DNA sequestration

Tone Sandal,[1] Klara Valyi-Nagy,[1,2] Virginia Spencer, [3] Robert Folberg,[1,2] Mina Bissell, [3] Andrew Maniotis, [1,2]

From the Department of Pathology, [1] University of Illinois at Chicago, Chicago, Illinois; the University of Illinois Cancer Center, [2] Chicago, Illinois, Lawrence Berkeley National Laboratory Life Sciences Division,[3] Berkeley, California.

Running title:
Tumor Plasticity, and Chromatin Organization

Key words:
3-D culture, breast cancer, chromatin, cAMP, extracellular matrix, fibronectin, genotype, PI3-Kinase, nucleus, signaling, tumor plasticity.

Abstract

The importance of microenvironment and context in regulation of tissue-specific genes is finally well established. DNA exposure to, or sequestration from, nucleases can be used to detect differences in higher order chromatin structure in intact cells without disturbing cellular or tissue architecture. To investigate the relationship between chromatin organization and tumor phenotype, we utilized an established 3-D assay where normal and malignant human breast cells can be easily distinguished by the morphology of the structures they make (acinus-like vs tumor-like, respectively). We show that these phenotypes can be distinguished also by sensitivity to AluI digestion where the malignant cells are resistant to digestion relative to non-malignant cells. Reversion of the T4-2 breast cancer cells by either cAMP analogs, or a phospatidylinositol 3-kinase (P13K) inhibitor not only reverted the phenotype, but also the chromatin sensitivity to AluI. By using different cAMP-analogs, we show that the cAMP-induced phenotypic

reversion, polarization, and shift in DNA organization act through a cAMP-dependent-protein-kinase A-coupled signaling pathway. Importantly, inhibitory antibody to fibronectin also reverted the malignant phenotype, polarized the acini, and changed chromatin sequestration. These experiments show not only that modifying the tumor microenvironment can alter the organization of tumor cells but also that architecture of the tissues and the global chromatin organization are coupled and yet highly plastic.

Introduction

We have shown previously that the degree of malignancy, the organization of cytoskeleton, and the composition of the extracellular matrix (ECM) influence chromatin structure (Maniotis et al., 2005). We found that the DNA of cultured cell lines from malignant tumors, transformed fibroblasts harboring 3 oncogenes, and cells collected from human tumors were more resistant to nucleases compared to DNA from normal or nonmalignant and weakly malignant cells. In addition, cells with the same genotype exhibit different degrees of DNA sequestration and exposure when cytoskeletal components were selectively disrupted, or when they were cultured on different ECM components (Maniotis et al., 2005).

Without viral insertion, additional deletion, or mutation of genes, it is possible to revert malignant tumor cells into cells those behave phenotypically normal. On 2-dimensional (2-D) surfaces, malignant cells can be induced by addition of cAMP to cease blebbing, form an organized cytoskeleton, and develop contact-inhibited monolayers (Krystosek et al., 1990; Puck et al., 2002). In a 3-dimensional (3-D) tissue culture system, it is possible to induce breast cancer cells to form normal tissue structures resembling breast acini (Wang et al., 2002; Weaver et al., 2002; Weaver et al., 1997). In experimental animal models, teratocarcinoma cells placed into mammalian embryos (Mintz and Illmensee,

1975), avian embryos transformed with Rous sarcoma virus (Dolberg and Bissell, 1984), and metastatic, aneuploid melanoma cells placed in chick embryos (Kulesa et al., 2006) develop into normal structures and tissues, and do not form tumors as they would in the adult organisms. These findings demonstrate that the phenotypes of malignant, metastatic, or transformed cells are highly plastic and regulated by the environment in which they are placed. The mechanisms underlying these phenotypic plasticities are not understood. In addition, it is not known if changes in cell phenotype are accompanied by epigenetic changes in DNA organization.

Here we have employed a well-characterized, phenotypically breast tumor model system in 3-D (Bissell and Labarge, 2005; Petersen et al., 1992; Weaver et al., 1997) to determine whether the transition of a tumor cells from disorganized clusters to organized, polar acinus-like structures is accompanied by global epigenetic changes in chromatin structure that could be quantified using the degree of resistance to DNA-degrading enzymes. We show that the organization of DNA in a malignant, mammary epithelial cell line follows tissue architecture. Moreover, tissue phenotype, and DNA organization are plastic, and reversible. We take advantage of these observations to test the following question: Through manipulation of single molecules in the microenvironment, is it possible to reversibly control DNA exposure/sequestration, cell polarity, tumor morphology, and ultimately, tumor behavior?

Materials and Methods

Cell lines and Cell culture

MCF10A, a nonmalignant human breast epithelial cells was obtained from American Type Culture Collection (Rockville, MD); the spontaneously transformed and malignant human breast epithelial line, HMT-3522 T4-2, was isolated by (Briand et al., 1996) and

was from the laboratory of Mina J Bissell at Lawrence Berkley National Lab. MCF10A cells were maintained in DMEM/F12 (Biowhittaker, Inc. Walkersville, MD) containing 20 ng/mL EGF (Calbiochem, Corp, San Diego, CA), 1.4 x 10^{-6} M hydrocortisone (BD Bioscience, San Jose, CA), 0.1 ng/mL Cholera toxin (Sigma, St Louis, MO), 10 X 10^{-6} g/mL human Insulin (Calbiochem Corp.), 2 mM Glutamine L, 5% horse serum (Fisher, Ontario, Canada) and penicillin/streptomycin. HMT-3522 T4-2 cells were routinely grown in H14 medium without 10 ng/ml EGF on Vitrogen-coated plates (Biowhittaker, Inc. Walkersville, MD) as described (Weaver et al., 2002).

3-D Cultures

Three-dimensional cultures were prepared based on previously described protocols (Debnath et al., 2003; Weaver et al., 1997) with some modifications: Cover slips (18 x 18 mm) were coated with 120 µl of Reduced growth factor Matrigel (BD Bioscience, San Jose, CA). Single cell suspensions (0.5 - 1.0 X 10^5 cells per slip) were seeded on top of polymerized Matrigel, incubated for 30 min and over-laid with 2.5 ml of culture medium containing no EGF or serum. Cells were overlaid with medium containing 2% Matrigel. Cultures were grown for days indicated in figure legends, adding new medium every third day.

DNA Digestion Assay

Cell smear assays were performed as described previously (Maniotis et al., 2005). Briefly, monolayer cultures grown on 10 cm dishes (70-90 % confluent) were mechanically dislodged or trypsinized off the plate, collected by centrifugation, re-suspended in serum-free DMEM. A drop (20 µl) of the suspension was placed on a glass slide and dried for 1 hour. DNA digestion was initiated by adding 50 µl of serum free

DMEM containing 0.5 µl of 10 U/µl AluI (Promega, San Luis Obispo CA) restriction enzyme (5 U per smear) for 30-90 min, and terminated by adding 1 µg/ml Ethidium bromide (Fisher Scientific) to stain DNA. Nuclei were observed and photographed using a Leica inverted fluorescent microscopy (Leica, Bannockburn, IL).

DNA digestion was performed on cells in 3-D cultures grown for 14 days. In preliminary experiments, we first determined both the time and concentration of AluI required for DNA digestion taking into account that large aggregates of T4-2 contains more DNA than smaller MCF10A acini. Eight hours digestion using 60 Units of AluI was sufficient for complete digestion of MCF10A organized acini. The T4-2 aggregates still exhibited partial resistance to digestion after 36 hours of digestion using a total of 600 Units AluI (added 200 Units every 12 hour) suggesting that the difference in DNA digestion is not due to differences in the amount of DNA contained in the 3-D cultures

Both Triton X-100 (0.1%) and NP-40 (0.1%) were tested as detergents to permeabilize cells in 3-D cultures to explore if the detergent *per se* affected DNA digestion. No difference in sensitivity to DNA digestion was observed using either one of these detergents, however NP-40 restored the normal morphology (round shape) of nuclei better than Triton X100 making it easier to evaluate the results. Cells in 3-D cultures grown 14 days were first permeabilized for 15 min with 0.1% NP-40, rinsed gently 3 times in PBS and incubated with serum-free DMEM containing AluI restriction enzyme (Promega, San Luis Obispo CA) for 24h in an incubator at 37˚C. Three-dimensional cultures of MCF10A acini, HMT-3522 T4-2 aggregates and HMT-3522 T4-2 revertants were digested with 20 µl AluI (100 U/ml of media) added twice (total 400U/reaction) within a 24-hour incubation period. Ethidium bromide (0.5 µg/ml) was added to label DNA at the termination of the reaction. Nuclear fluorescence was photographed with a

Leica inverted fluorescent microscope. Parallel cultures in each experiment were stained with Trypan blue (MP Biomedicals, Ohio) to confirm complete permeabilization.

Flow Cytometry

Cells from monolayer cultures of MCF10A and T4-2 were harvested either by scraping or trypsinization, diluted in PBS, and collected by centrifugation. The pellet was re-suspended in 0.1% NP-40 and incubated for 1 min at room temperature to permeabilize the cells, followed by a second spin to wash away detergent. Pellets were re-suspended in 0.5 ml of regular DMEM with 65 U of AluI and incubated for 1h under rotation at 37˚C. Propidium iodide (1 µg/ml, Invitrogen/Molecular Probes, Carlsbad, CA) was added directly to each reaction at its conclusion, and the cell suspension was filtered through flow tubes with a filtered cartridge before flow cytometric analysis.

After treating T4-2 non-reverted and reverted cells from 3-D cultures with Dispase (BD Bioscience, San Jose) for 30 min at 37˚C to degrade Matrigel proteins, cells were harvested into 15 ml Falcon tubes and re-suspended. To disperse the structures into single cell suspension, Trypsin (0.25%) was added (200 ul) and incubated for 5 min at 37°C. Single cells were collected by centrifugation and re-suspended in PBS containing 1µg/ml propidium iodide (Invitrogen/Molecular Probes, Carlsbad, CA). Cell suspensions were filtered through Flow tubes with a filtered cartridge and taken to flow cytometric analysis. All analyses were performed on a FACS Calibur (BD Bioscience, San Jose) equipped with a 488 laser for forward and side scatter, and 520, 575 and 675 nm detectors. Each run ended at 10,000 counts and was analyzed using FACS dot-plots and histograms. Propidium iodide signal represents labeled DNA, and signal intensity of undigested DNA (roughly corresponding to fluorescent intensity 10^2-10^4) was gated as

M2. Lower signal intensity representing digested DNA (shorter DNA fragments) was gated as M1.

Phenotypic Tumor Reversion with PI3K inhibitor and or dibutyryl-cAMP

Cells were seeded on Matrigel as described above, overlaid with 2.5 ml of growth medium containing 8 μM PI3K inhibitor LY294002 (Calbiochem/EMD Biosciences, Inc.) San Diego, CA), or a combination of 6 μM LY294002 and 1 mM N^6-dibutyryl-cAMP (Sigma-Aldrich St Louis, MO)). Cultures were maintained for 14 days with addition of new drugs every third day. No toxicity was observed in either normal or tumorigenic 3-D cultures of mammary epithelial cells at these drug concentrations. Dibutyryl-cAMP analog, in addition to elevating cAMP within the cell, metabolizes to butyrate, which alone is known to have distinct biological effects. However sodium butyrate, in concentrations ranging from 1-2mM, did not induce tumor reversion when added to the T4-2 cell cultures, thus eliminating a possible butyrate effect involved in tumor reversion. In experiments testing cAMP analog specificity and tumor reversion, cells were seeded as above and overlaid with medium containing either 0.5 mM 8-CPT-2´-O-Me-cAMP (BioLog Life Science, Bremen, Germany) or 0.5 mM N^6-Monobutyryl-cAMP (BioLog Life Science).

Phenotypic Tumor Reversion with Antibodies to Extracellular Matrix Proteins

Cells were seeded on Matrigel as described above, and overlaid with 2.5 ml medium containing one of the following antibodies:rabbit anti-human fibronectin (A0245, Dako, Carpineria, CA, 1:100 dilution), mouse anti-human laminin (Lam-89, Sigma-Aldrich, St Louis, MO, 1:100 dilution), mouse anti-human Collagen IV (CIV22, Dako, Carpineria, CA, 1:100 dilution), rabbit anti-human Collagen I (CL50111AP, Cedarlane, Hornby,

Ontario, 1: 100 dilution) and mouse anti-human gamma-tubulin (Sigma-Aldrich St Louis, MO). The cultures were fed every third day by overlay with 1 ml of medium containing fresh antibody.

Immunofluorescence Microscopy

Cells were cultured on top of a Matrigel-covered cover slip for 14 days as described above. Cover slips were washed 3 times with cytoskeleton extraction buffer (50 mM HEPES, 300 mM sucrose, 100 mM KCl, 5 mM MgCl2, 5 mM EDTA, 0.5 % Triton X-100, containing 1 mM sodium orthovanadate, 20 mM sodium fluoride and 20 µl/ml protease inhibitor cocktail from Sigma-Aldrich for 3 sec, rinsed with 1 X PBS and fixed in 100% ice-cold methanol (5 min in –20˚C) followed by 5 min incubation in ice-cold 100% acetone. Cells were rinsed 3 times in 1 x PBS and incubated over night at 4˚C with mouse anti-human β_4 intergrin (clone E31) at a 1:200 dilution (Chemicon, Temecula, CA) or mouse antį-β-catenin (clone 14) at 5 µg/ml dilution (BD Transduction Labs, San Jose, CA). Slides were washed 3 times for 2 - 5 min, incubated with a 1:200 dilution of goat anti-mouse secondary antibody conjugated to Alexa Fluor 546 (Molecular Probes) for 30 min at, washed 3 x (as above) and mounted on glass slides in Vectashield mounting medium (Vector Laboratories, Burlington, CA). Control cultures for all experiments were treated with the same concentration of non-specific rabbit IgG (Cat. No. ab27478; Abcam, Cambridge, MA). The cultures were fed every third day by overlay of 1ml medium containing fresh antibody.

Laser Scanning Confocal Microscopy

Confocal images were taken on a Zeiss LSM510 laser scanning microscope (Carl Zeiss Micro Imaging Inc., Thornwood, New York, USA) using Incident Light Fluorescence and

Differential Interference Contrast (DIC) with 25X and 63X water immersion objectives. Argon laser was applied for red fluorescence (AlexaFluor 546 and $EtBr_2$ at 543 nm wavelength) and UV laser for blue fluorescence (DAPI at 405 nm wavelength). Images were captured using LSM Software Reliase 2.5 on a standard high-end Pentium PC.

Results

Phenotypic reversion of tumorigenic T4-2 cells

The behavior of T4-2 tumorigenic cells in 3-D culture conditions was compared with normal MCF10A breast epithelial cells. After 10 to 14 days, MCF10A cells formed polarized acini (Figure 1 A) with the nuclei arranged circumferentially around the hollow interior. β4-integrin was distributed in a circular ring, facing the extracellular matrix environment (Figure 1B) and β-catenin was identified internally on cell surfaces between different cells comprising the multi-cellular acini (Figure 1C). By contrast, within 10 to 14 days, T4-2 cells developed into disorganized aggregates (Figure 1D) that were considerably larger than polarized structures formed by MCF10A cells (note differences in scale bar sizes) (Figure 1). In the disorganized T4-2 aggregates, β4-integrin distribution was observed on cell surfaces facing all directions, both between cells and on surfaces facing the extracellular environment (Figure 1E). Also, in the disorganized T4-2 aggregates, β-catenin was distributed in and between most of the cells (Figure 1F). Compared to the architecture of MCF10A acini, the disorganized T4-2 aggregates appeared to exhibit complete loss of polarization.

Tumorigenic T4-2 cells can be induced to develop into architecturally-normal acinus-like structures *in vitro* when cultured in the presence of a PI3K inhibitor, and these acinus-like structures exhibit non-tumorigenic behavior in nude mice (Wang et al., 2002; Weaver et al., 2002; Weaver et al., 1997). We confirmed the *in vitro* reversion of

tumorigenic T4-2 cells by culturing on Matrigel in the presence of 8 μM PI3K inhibitor LY294002 (not shown) consistent with the findings of (Liu et al., 2004; Wang et al., 2002; Weaver et al., 2002; Weaver et al., 1997). We also obtained phenotypic reversion using dibutyryl-cAMP at a concentration of 1mM (not shown), consistent with previous observations of phenotypic tumor reversion of monolayer cultures (Krystosek et al., 1990).

A combination of 6 μM LY294002 PI3K inhibitor and 1mM dibutyryl-cAMP induced the formation of reverted structures most similar to the acini formed by MCF10A cells in terms of size, polarization, and lumen formation (Figure1). In the acini formed by the reverted T4-2 cells, a dense ring of β4-integrin surrounded each spheroid (Figure 1H), similar to the ring of integrin formed around normal MCF10A structures (Figure 1B). In addition, β-catenin was redistributed from a disorganized haphazard pattern in the non-drug-treated T4-2 aggregates, to a lace-like or stellar pattern of the drug treated structures (compare Figure 1F and I) that closely resembled β-catenin distribution in MCF10A cells in 3D culture conditions (compare Figure 1C and I). Moreover, acinus-like structures formed by T4-2 cells exposed to the combination of LY294002 PI3K inhibitor and dibutyryl-cAMP, were hollow, similar to the MCF10A acini (see Figure 1B and H). Therefore, because of the degree of fidelity we observed in the architecture of the revertants compared to normal MCF10A structures when using the combination of 6 μM LY294002 PI3K inhibitor and 1mM dibutyryl-cAMP, this treatment was employed as our standard protocol to consistently induce revertants exhibiting acinus-like structures with size and phenotype most similar to MCF10A acini.

Differential DNA digestion in normal versus tumorigenic mammary epithelial cells grown in 2-D cell cultures

Consistent with our reported observations (Maniotis et al., 2005), a MCF10A cell-smear assay showed that the DNA in these cells was extensively digested after a 1.5 hour exposure to AluI restriction enzyme (Figures 2A, B). By contrast, DNA in the nuclei of malignant T4-2 cells appeared to be mostly undigested after 1.5 hours exposure to AluI (Figures 2C, D). To confirm these qualitative observations, DNA digestion was quantified by flow cytometry (see Materials and Methods). Under these conditions, a shift in the DNA profile of MCF10A cells was observed within 60 min of AluI digestion (Figure 2 E and F), while less of a change was observed for tumorigenic T4-2 cells treated in the same manner (Figure 2G and H). The DNA profile for non-treated and AluI-treated MCF10A and T4-2 cells was collected from 5 separate DNA digestion experiments and averaged (Figure 2I). Figures 2J and 2K demonstrate the degree of AluI digestion in MCF10A and T4-2 cells that were subjected to flow cytometry analysis.

Differential DNA digestion in normal versus tumorigenic mammary epithelial cells grown in 3-D cell cultures

To explore the sensitivity of DNA to AluI restriction enzyme of cells exhibiting 3-D architectural structure we developed an assay for the digestion of cells in 3-D culture conditions by AluI (see Materials and Methods). MCF10A epithelial cells and T4-2 tumorigenic breast carcinoma cells were cultured for 14 days on Matrigel and allowed to form small acinus-like structures or large disorganized aggregates, respectively (see Figure 1). Following permeabilization with 0.1% NP-40 for 10 minutes, nuclei and morphology remained intact (Figure 2L, M, N, O, P and Q) in the 3-D cultures of MCF10A and transformed T4-2 respectively. Furthermore, these conditions allowed sufficient permeabilization for complete uptake of Trypan blue in small acini or acinus-

like structures of MCF10A, reverted T4-2 (Figure 2R and S) and large transformed T4-2 aggregates (Figure 2T), indicating that the 3-D structures were completely permeabilized.

After incubation with AluI for 24h, the chromatin in MCF10A acini was completely digested (Figure 2U and Y). By contrast, chromatin in T4-2 cells forming disorganized aggregates resisted digestion in the same time period under identical conditions (Figure 2V and Z). Thus, the chromatin of MCF10A cells assembled into acini was far more sensitive to AluI digestion than the chromatin of T4-2 cells assembled into disorganized multicellular aggregates (compare high magnification images Figures 2Y and Z).

Reversible manipulation of phenotype and DNA sequestration

We applied the reversible T4-2 system to test if there is a differential sensitivity to Alu I in DNA of reverted T4-2 cells forming acinis-like structures, compared to DNA in transformed T4-2 cells forming disorganized aggregates. Strikingly, under identical AluI digestion conditions, we observed that DNA in T4-2 disorganized aggregates (Figure 3A) was far more resistant to digestion than the DNA in T4-2 cells induced to form acinus-like structures (revertants), by either PI3K inhibitor (not shown) or the PI3K inhibitor plus dibutyryl-cAMP (Figure 3B). The extent of differential digestion is clearly illustrated by images collected at a higher magnification (Figures 3E and F). Both T4-2 revertants and aggregate structures displayed an intact morphology as revealed by corresponding DIC images (Figure 3G and H). These results demonstrate for the first time that phenotypic tumor reversion is accompanied by a significant shift in chromatin sequestration.

Exposure of T4-2 cells to PI3K inhibitor plus dibutyryl-cAMP (Figure 4B) resulted in the formation of organized acinus-like structures (Figures 3 C and D) that harbored DNA,

which completely digested with AluI restriction enzyme. In contrast, the chromatin from non-reverted, disorganized T4-2 cell aggregates was more resistant to digestion. The removal of PI3K inhibitor and dibutyryl-cAMP over a 14 day period caused the reverted T4-2 acinus-like structures to gradually grow larger, and become disorganized to a point where they were phenotypically identical to control, non-reverted T4-2 cells aggregates (Figure 3I, J, K and Figure 1 and 2). As the reverted T4-2 cells changed morphologically from organized spheroids (day 0) to disorganized spheroids (day 7) and to disorganized aggregates without any evidence of polarity (day 15), DNA became more resistant to digestion with AluI restriction enzyme (Figure 3L, M, N, O, P, Q). Quantification using flow cytometry confirmed the visual comparisons of DNA digestion experiments (Figure 3R). Taken together, reversible manipulation of 3-D cultures from a tumor-like architecture to a normal architecture, and back again, was consistently accompanied by reversible changes in DNA sequestration.

Manipulation of morphology, polarization, and chromatin sensitivity to DNA digestion specifically involves a Protein Kinase A (PKA) coupled signal

Dibutyryl-cAMP has been reported to induce reverse transformation of a number of transformed cell lines grown in monolayer (Krystosek et al., 1990; Puck et al., 2002). Treatment with 1mM dibutyryl-cAMP was reported in 12 different tumorigenic cell lines to restore normal morphology and sensitivity to nuclear chromatin digestion by DNase I. Cyclic AMP has traditionally been thought to act exclusively through the cAMP-dependent protein kinase A (Ashall et al., 1988; Walsh et al., 1968), and effects of cAMP on tumor reversion have been attributable to activation of PKA (Kim et al., 2000; Schonberg et al., 1983). However, the action of intracellular cAMP is not only mediated by PKA, but also by a newly recognized family of cAMP-binding proteins designated as

cAMP-regulated guanine nucleotide exchange factors (also known as *Epac*) (de Rooij et al., 1998; Kawasaki et al., 1998).

To discriminate between Epac and PKA coupled signals, we tested specific cAMP analogs for their ability to revert T4-2 cells in 3-D cultures. Monobutyryl-cAMP which is a poor agonist for Epac but a potent PKA activator (Christensen et al., 2003; Kopperud et al., 2003), phenotypically reverted the T4-2 cells into organized acinus-like structures (Figure 4A) as was seen for T4-2 cells treated with PI3K inhibitor plus dibutyryl-cAMP (Figure 2B). Beta 4-integrin distribution within the monobutyryl-cAMP-reverted acinus-like structures appeared on the cell surfaces facing the microenvironment and these reverted structures appeared to be hollow in the center, confirming polarized organization (Figure 4C and D). Furthermore, the nuclei of these reverted T4-2 spheroids were also sensitive to DNA digestion by AluI (Figure 4E and F). Parenthetically, the 8-CPT-2P-O-Me-cAMP analog (a selective and strong agonist for Epac (de Rooij et al., 1998)) did not revert tumorigenic T4-2 cells into polarized acinus-like structures (Figures 4G-H): β4-integrin was randomly distributed on cell surfaces throughout the disorganized cell aggregates (Figure 4 I and J), and the nuclei were resistant to DNA digestion by AluI (Figure 4K and L).

Antibody interference of extracellular matrix components drives phenotypic tumor reversion, induces polarization, and exposes sequestered DNA

We next aimed to determine if changes in the interaction between T4-2 cells (forming either aggregates or reverted acinus-like structures) and the ECM influenced the phenotype, structural polarity, and DNA organization. T4-2 cells were cultured in Matrigel with antibodies targeting individual ECM components including: fibronectin (FN), collagen I (Col I), collagen IV (Col IV), and laminin (LM) (Table 1 and Figures 5A-D).

The treatment of T4-2 cells with each of these antibodies induced changes in phenotypic behavior that were evident as early as 6-7 days (data not shown) and more pronounced by day 14 when compared to cultures treated with IgG as a control. (Figure 5E). Anti-FN antibody treatment completely reverted the T4-2 cells to acinus-like morphology (Figure 5A), indistinguishable from revertants produced via the combination of PI3K inhibitor and dibutyryl-cAMP or with monobutyryl-cAMP analog alone (compare with Figure 5A with Figure 4A and B). Cells grown in the presences of anti-Col I antibody and anti–Col IV antibody obtained a spherical morphology (Figure 5B and C). Anti-LM treated cultures tended to exhibit horizontal plaque-like structures (Figure 5D). We specifically tested in a separate series of experiments if sodium azide may have a synergistic affect on tumor reversion since the antibody solvent contains low concentrations of sodium azide. The results of these experiments demonstrated that sodium azide had no effect by itself or in combination with control antibodies used in these experiments (data not shown).

We next explored if these antibody-induced morphological changes were accompanied by changes in polarization. To test this, T4-2 cells grown on Matrigel for 14 days in the presence of various antibodies were immunostained with anti- β4-integrin antibody. In this experiment, T4-2 revertants were produced via exposure to PI3K inhibitor and dibutyryl-cAMP to serve as controls for normal acinus-like morphogenesis. (Figure 5F and F'). Remarkably, T4-2 cultures exposed to anti-FN antibody exhibited polarized hollow lumen, and β4-integrin was distributed on the acinus-like surfaces facing the ECM (Figure 5 G and G'), identical to the standard controls (Figure 5F), Anti-Col I antibody induced spherical structures, however, they did not appear hollow nor were they polarized as suggested by the random distribution of β4-integrin (Figure 5H and H'). Anti-LM antibody-treated cultures also did not appear to be polarized and exhibited long

strings of β4-integrin staining between the horizontal cell plaques (Figure 5I). Cells grown in the presence of non-specific IgG served as a negative control with respect to polarization and behaved similar to untreated cultures (Figure 5J and K).

We next wanted to determine the nuclease sensitivity of DNA from cells that assumed polarized structures after treatment with an anti-FN antibody and to compare this sensitivity with that of cells treated with an anti-laminin antibody that induced the smallest degree of morphological reversion. In this experiment, we included untreated, transformed T4-2 aggregates and PI3K inhibitor/dibutyryl-cAMP- reverted T4-2 acinus-like structures as controls for sequestered and exposed chromatin, respectively (Figure 5L-O).The nuclei of anti-fibronectin-revertants harbored completely digested DNA after 24h of digestion with AluI (Figure 5P-S), similar to T4-2 revertants (Figure 5 N and O) obtained by the standard protocol. The cells in the plaque-like anti-LM treated cultures, by contrast, harbored chromatin that was resistant to 24 hours of AluI digestion (Figure T-W), similar to chromatin in the transformed T4-2 aggregates (Figure 5L).

Discussion

We have shown that the DNA of non-malignant breast epithelial cells that form polarized acini, are exposed to AluI digestion, while, tumorigenic cells that form disorganized, non-polarized aggregates, exhibit profound sequestration of their DNA under identical enzymatic digestion conditions. Tumorigenic T4-2 cells induced to form polarized acinus-like structures displayed a level of sensitivity to AluI that was comparable to that observed in normal MCF10A cells when assembled into acini. Thus, the act of T4-2 cell polarization and assembly into an acinus-like structure shifted the chromatin organization of these cells, causing previously sequestered DNA to assume a more open conformation with increased accessibility to AluI.

Also, when established reverted T4-2 acinus-like structures are released from agents that induce polarity, they grow into disorganized, unpolarized, aggregates. This shift from a reverted to a tumorigenic morphology is accompanied by a shift in chromatin organization from an exposed to a sequestered state. From these results, we conclude that chromatin organization is coupled to tissue architecture, and can be reversibly manipulated. More specifically, chromatin organization is linked to cell polarity, and the 3-D organization of cells in an extracellular environment.

Many different *in vitro* and *in vivo* observations support the fact that transformations in phenotype and DNA sequestration are not enzymatic artifacts (Maniotis et al., 2005).
For instance, we previously showed that the DNA in human cancer cells is tightly packaged *in vitro*, making it less susceptible to digestion by restriction enzymes (Maniotis et al., 2005). Most importantly, touch preparations made from comparing human lesions with their margins in the normal tissue, all demonstrate that the more invasive the cancer, the better its DNA is protected from restriction enzyme cleavage (Maniotis et al., 2005). Therefore, enhanced DNA protection has now been observed in many different types of cancer, and is reversible, suggesting that DNA re-arrangements as described here may be a universal feature of malignant cells. The fact that sequestration of DNA, and the molecular consequences of such, serve as a physical marker for malignancy, may be applicable in other types of cancer detection as well. Therefore chromatin organization analysis may be a supplement for current methods of cancer diagnostics which detect chemical markers that are highly variable from tumor to tumor and from patient to patient, or which are highly specific for certain types of tumors.

In devising the most optimal conditions for generating polarized acinus-like structures from T4-2 cells, we discovered that a cocktail of two reagents that can each alone revert T4-2 cells produced the most consistent development of acinus-like, polarized structures. These reverted structures resembled the polarized acini generated by non-malignant MCF10A cells. This finding supports previous studies using PI3K inhibitor (Wang et al., 2002) or an analog of dibutyryl-cAMP for tumor reversion (Krystosek et al., 1990; Puck et al., 2002). In addition, we show for the first time that these reagents are able to revert cancer cells in a 3-D context. Biochemically, the action of intracellular cAMP can be attributed to activation of at least two intracellular substrates, PKA and EPAC (de Rooij et al., 1998; Kawasaki et al., 1998). Using specific cAMP-analogs that discriminate between the activation of these substrates (Christensen et al., 2003; Kopperud et al., 2003), we found that the reversion of T4-2 morphology, polarity, and AluI sensitivity exclusively involves a PKA-coupled signal.

Unraveling the complexity of DNA packaging or sequestration *in its native state* within the intact cell nucleus may suggest a new possible mechanistic explanation of how eukaryotic genes are turned on or off, and how they are reversibly expressed or suppressed. From a mechanistic point of view, these experiments employing in situ DNA digestion with AluI indicate that higher order structure of native chromatin is organized such that the sequestration and exposure of DNA is linked to cytoarchitecture (cell polarity, cell shape, organoid 3-D architecture). Because DNA, the substrate, must be exposed to AluI, the enzyme, in order to be digested, the AluI insensitive revertants (DNA sequestered), or the AluI sensitive tumorigenic (DNA exposed) phenotypes suggests that proteins organizing higher order chromatin structure are capable of reversibly enveloping the DNA as a tightly-wrapped spring (resembling a sleeve), in which the DNA can be reversibly exposed or sequestered (Maniotis et al., 2005). Such

an hypothesis provides a mechanistic picture of how higher order chromatin in the living state may grouped together, to expose or sequester DNA in regular patterns. This may in turn account for specific malignant cancer, non-malignant cancer, or normal gene expression and phenotypic expression types.

When tumorigenic viruses, or when highly invasive tumor cells are placed into embryos, tumors do not form, which suggests that the behavior of cancer is contextual (Dolberg and Bissell, 1984; Kulesa et al., 2006; Mintz and Illmensee, 1975). These studies demonstrate that when highly invasive tumor cells are placed into the complex milieu of soluble and insoluble factors within the embryo, they become “regulated,” to behave as normal cells, without causing cancer in the mosaic organism that develops. If tumor cells are implanted early enough during embryogenesis, some of the tumor cells are passed down through the germ line, and to the mosaic organism’s descendents without causing cancer in these mosaic organisms (Mintz and Illmensee, 1975). Importantly, context-regulation of cancer cells in the embryonic environment occurs even when the cancer cells have already metastasized from their primary tumor site (Kulesa et al., 2006). This suggests that context-regulation of cancer cells is possible despite deregulation of proteins, of cell structure, of cell cycle, of telomerase activity, and occurs independent of mutations, aberrations of oncogenes, and aneuploidy.

It is known that the ECM by itself can provide signals that are relayed from integrin receptors on the cell surface to the nucleus by (Ingber et al., 2003; Maniotis et al., 1997; Roskelley and Bissell, 2002). Therefore, we explored if tumor reversion, and the accompanying chromatin reorganization, could be obtained by interfering only with specific cues from the ECM using antibodies to proteins found in our malignant tumor samples. In particular, we specifically targeted those ECM components that have been

reported to be highly expressed by various tumors (Ioachim et al., 2002; Ioachim et al., 2005; Lin et al., 2005). The different antibodies used, all induced profound changes in the development and the resulting morphology of T4-2 structures (see Table 1 and Figure 5). Of key importance, the structures induced by anti fibronectin exhibited chromatin that was exposed in an identical fashion to chromatin of normal acini and chromatin in acinus-like structures produced by cAMP and PI3K inhibitor. By contrast, and at the other extreme, the anti laminin induced structures (large horizontal plaque-like structures) exhibited chromatin that was sequestered.

Here we have shown that placing T4-2 cells in the context of a laminin-rich matrix in the presence of a single component such as anti-fibronectin induces complete phenotypic reversion from normal to tumorigenic phenotype, and from DNA being in a sequestered state or an exposed state, and that these states are reversible. These observations suggest that the components of the tumor microenvironment can be identified, isolated, and perhaps therapeutically exploited, as indicated in the reversion obtained with a single molecular species such as anti-fibronectin.

Specific isoforms of fibronectin that are normally expressed in fetal tissue (George et al., 1997; George et al., 1993), and rarely expressed in adult tissue, have been detected in different cases of human cancer (Schor et al., 1988). In addition, the B-isoform of fibronectin (EDB-fibronectin) plays a role in cellular transformation and tumor pathogenesis (Castellani et al., 1994; Kaczmarek et al., 1994; Labat-Robert, 2004; Midulla et al., 2000; Schor et al., 1986; Zardi et al., 1987), and a truncated isoform of fibronectin referred to as fetal migration stimulatory factor has been detected in the serum of 90% of breast cancer cases (Picardo et al., 1991), as well as in other human cancers (Durning et al., 1984; Schor et al., 2003; Schor et al., 1986). Elucidating the

mechanisms through which ECM components influence tumor cell and DNA organization may lead to the identification of new potential targets for cancer therapy.

In summary; 1) information conveyed from the extracellular matrix environment controls tissue phenotype, cellular and organoid, polarity, and DNA sequestration or exposure 2) shifts in cellular polarity and chromatin organization are concomitant events, and 3) agents targeting multiple signaling pathways (eg. PI3K, PKA, and fibronectin) evoke identical phenotypes (and chromatin exposure). The causal determinants of indolent or malignant cancer cell behavior and chromatin organization appear to be epigenetic rather than genetic in nature, and these signaling pathways can be manipulated from outside of tumor cells by selecting specific molecular targets within the extracellular matrix.

Acknowledgement
We gratefully thank Dr. M. Chen at the Research Resource Center (University of Illinois at Chicago) for expert assistance with confocal and helpful discussions. We specially thank Professor Stein Ove Doseland at the Department of Biomedicine (University of Bergen, Norway) for providing cAMP analogs and for helpful advice and discussions.
We dedicate this work in memory of Dr. Theodore Puck.

This work was supported by Department of Energy Grant DEAC03-76SF0098, grant EY10457 from the National Institutes of Health, and grants from the Norwegian Cancer Society.

Ashall, F., Sullivan, N. and Puck, T.T. (1988) Specificity of the cAMP-induced gene exposure reaction in CHO cells. *Proc Natl Acad Sci U S A*, **85**, 3908-3912.

Bissell, M.J. and Labarge, M.A. (2005) Context, tissue plasticity, and cancer: are tumor stem cells also regulated by the microenvironment? *Cancer Cell*, **7**, 17-23.

Briand, P., Nielsen, K.V., Madsen, M.W. and Petersen, O.W. (1996) Trisomy 7p and malignant transformation of human breast epithelial cells following epidermal growth factor withdrawal. *Cancer Res*, **56**, 2039-2044.

Castellani, P., Viale, G., Dorcaratto, A., Nicolo, G., Kaczmarek, J., Querze, G. and Zardi, L. (1994) The fibronectin isoform containing the ED-B oncofetal domain: a marker of angiogenesis. *Int J Cancer*, **59**, 612-618.

Christensen, A.E., Selheim, F., de Rooij, J., Dremier, S., Schwede, F., Dao, K.K., Martinez, A., Maenhaut, C., Bos, J.L., Genieser, H.G. and Doskeland, S.O. (2003) cAMP analog mapping of Epac1 and cAMP kinase. Discriminating analogs demonstrate that Epac and cAMP kinase act synergistically to promote PC-12 cell neurite extension. *J Biol Chem*, **278**, 35394-35402. Epub 32003 Jun 35320.

de Rooij, J., Zwartkruis, F.J., Verheijen, M.H., Cool, R.H., Nijman, S.M., Wittinghofer, A. and Bos, J.L. (1998) Epac is a Rap1 guanine-nucleotide-exchange factor directly activated by cyclic AMP. *Nature*, **396**, 474-477.

Debnath, J., Muthuswamy, S.K. and Brugge, J.S. (2003) Morphogenesis and oncogenesis of MCF-10A mammary epithelial acini grown in three-dimensional basement membrane cultures. *Methods*, **30**, 256-268.

Dolberg, D.S. and Bissell, M.J. (1984) Inability of Rous sarcoma virus to cause sarcomas in the avian embryo. *Nature*, **309**, 552-556.

Durning, P., Schor, S.L. and Sellwood, R.A. (1984) Fibroblasts from patients with breast cancer show abnormal migratory behaviour in vitro. *Lancet*, **2**, 890-892.

George, E.L., Baldwin, H.S. and Hynes, R.O. (1997) Fibronectins are essential for heart and blood vessel morphogenesis but are dispensable for initial specification of precursor cells. *Blood*, **90**, 3073-3081.

George, E.L., Georges-Labouesse, E.N., Patel-King, R.S., Rayburn, H. and Hynes, R.O. (1993) Defects in mesoderm, neural tube and vascular development in mouse embryos lacking fibronectin. *Development*, **119**, 1079-1091.

Ingber, D.E., Alenghat, F.J., Danen, E.H. and Sonnenberg, A. (2003) Tensegrity I. Cell structure and hierarchical systems biology

Mechanotransduction: all signals point to cytoskeleton, matrix, and integrins

Integrins in regulation of tissue development and function. *J Cell Sci*, **116**, 1157-1173.

Ioachim, E., Charchanti, A., Briasoulis, E., Karavasilis, V., Tsanou, H., Arvanitis, D.L., Agnantis, N.J. and Pavlidis, N. (2002) Immunohistochemical expression of extracellular matrix components tenascin, fibronectin, collagen type IV and laminin in breast cancer: their prognostic value and role in tumour invasion and progression. *Eur J Cancer*, **38**, 2362-2370.

Ioachim, E., Michael, M., Stavropoulos, N.E., Kitsiou, E., Salmas, M. and Malamou-Mitsi, V. (2005) A clinicopathological study of the expression of extracellular matrix components in urothelial carcinoma. *BJU Int*, **95**, 655-659.

Kaczmarek, J., Castellani, P., Nicolo, G., Spina, B., Allemanni, G. and Zardi, L. (1994) Distribution of oncofetal fibronectin isoforms in normal, hyperplastic and neoplastic human breast tissues. *Int J Cancer*, **59**, 11-16.

Kawasaki, H., Springett, G.M., Mochizuki, N., Toki, S., Nakaya, M., Matsuda, M., Housman, D.E. and Graybiel, A.M. (1998) A family of cAMP-binding proteins that directly activate Rap1. *Science*, **282**, 2275-2279.

Kim, S., Harris, M. and Varner, J.A. (2000) Regulation of integrin alpha vbeta 3-mediated endothelial cell migration and angiogenesis by integrin alpha5beta1 and protein kinase A. *J Biol Chem*, **275**, 33920-33928.

Kopperud, R., Krakstad, C., Selheim, F. and Doskeland, S.O. (2003) cAMP effector mechanisms. Novel twists for an 'old' signaling system. *FEBS Lett*, **546**, 121-126.

Krystosek, A., Puck, T.T., Ashall, F., Sullivan, N., Schonberg, S. and Patterson, D. (1990) The spatial distribution of exposed nuclear DNA in normal, cancer, and reverse-transformed cells

Specificity of the cAMP-induced gene exposure reaction in CHO cells

Resistance of Chinese hamster ovary cell chromatin to endonuclease digestion. I. Reversal by cAMP. *Proc Natl Acad Sci U S A*, **87**, 6560-6564.

Kulesa, P.M., Kasemeier-Kulesa, J.C., Teddy, J.M., Margaryan, N.V., Seftor, E.A., Seftor, R.E. and Hendrix, M.J. (2006) Reprogramming metastatic melanoma cells to assume a neural crest cell-like phenotype in an embryonic microenvironment. *Proc Natl Acad Sci U S A*, **103**, 3752-3757.

Labat-Robert, J. (2004) [Thirty years after fibronectin discovery: role in malignant transformation and in ageing]. *J Soc Biol*, **198**, 287-291.

Lin, A.Y., Maniotis, A.J., Valyi-Nagy, K., Majumdar, D., Setty, S., Kadkol, S., Leach, L., Pe'er, J. and Folberg, R. (2005) Distinguishing fibrovascular septa from vasculogenic mimicry patterns. *Arch Pathol Lab Med*, **129**, 884-892.

Liu, H., Radisky, D.C., Wang, F. and Bissell, M.J. (2004) Polarity and proliferation are controlled by distinct signaling pathways downstream of PI3-kinase in breast epithelial tumor cells. *J Cell Biol*, **164**, 603-612. Epub 2004 Feb 2009.

Maniotis, A.J., Chen, C.S. and Ingber, D.E. (1997) Demonstration of mechanical connections between integrins, cytoskeletal filaments, and nucleoplasm that stabilize nuclear structure. *Proc Natl Acad Sci U S A*, **94**, 849-854.

Maniotis, A.J., Valyi-Nagy, K., Karavitis, J., Moses, J., Boddipali, V., Wang, Y., Nunez, R., Setty, S., Arbieva, Z., Bissell, M.J. and Folberg, R. (2005) Chromatin organization measured by AluI restriction enzyme changes with malignancy and is regulated by the extracellular matrix and the cytoskeleton. *Am J Pathol*, **166**, 1187-1203.

Midulla, M., Verma, R., Pignatelli, M., Ritter, M.A., Courtenay-Luck, N.S. and George, A.J. (2000) Source of oncofetal ED-B-containing fibronectin: implications of production by both tumor and endothelial cells. *Cancer Res*, **60**, 164-169.

Mintz, B. and Illmensee, K. (1975) Normal genetically mosaic mice produced from malignant teratocarcinoma cells. *Proc Natl Acad Sci U S A*, **72**, 3585-3589.

Petersen, O.W., Ronnov-Jessen, L., Howlett, A.R. and Bissell, M.J. (1992) Interaction with basement membrane serves to rapidly distinguish growth and differentiation pattern of normal and malignant human breast epithelial cells. *Proc Natl Acad Sci U S A*, **89**, 9064-9068.

Picardo, M., Schor, S.L., Grey, A.M., Howell, A., Laidlaw, I., Redford, J. and Schor, A.M. (1991) Migration stimulating activity in serum of breast cancer patients. *Lancet*, **337**, 130-133.

Puck, T.T., Webb, P. and Johnson, R. (2002) Cyclic AMP and the reverse transformation reaction. *Ann N Y Acad Sci*, **968**, 122-138.

Roskelley, C.D. and Bissell, M.J. (2002) The dominance of the microenvironment in breast and ovarian cancer. *Semin Cancer Biol*, **12**, 97-104.

Schonberg, S., Patterson, D. and Puck, T.T. (1983) Resistance of Chinese hamster ovary cell chromatin to endonuclease digestion. I. Reversal by cAMP. *Exp Cell Res*, **145**, 57-62.

Schor, S.L., Ellis, I.R., Jones, S.J., Baillie, R., Seneviratne, K., Clausen, J., Motegi, K., Vojtesek, B., Kankova, K., Furrie, E., Sales, M.J., Schor, A.M. and Kay, R.A. (2003) Migration-stimulating factor: a genetically truncated onco-fetal fibronectin isoform expressed by carcinoma and tumor-associated stromal cells. *Cancer Res*, **63**, 8827-8836.

Schor, S.L., Haggie, J.A., Durning, P., Howell, A., Smith, L., Sellwood, R.A. and Crowther, D. (1986) Occurrence of a fetal fibroblast phenotype in familial breast cancer. *Int J Cancer*, **37**, 831-836.

Schor, S.L., Schor, A.M., Grey, A.M. and Rushton, G. (1988) Foetal and cancer patient fibroblasts produce an autocrine migration-stimulating factor not made by normal adult cells. *J Cell Sci*, **90**, 391-399.

Walsh, D.A., Perkins, J.P. and Krebs, E.G. (1968) An adenosine 3',5'-monophosphate-dependant protein kinase from rabbit skeletal muscle. *J Biol Chem*, **243**, 3763-3765.

Wang, F., Hansen, R.K., Radisky, D., Yoneda, T., Barcellos-Hoff, M.H., Petersen, O.W., Turley, E.A., Bissell, M.J., Wang, F., Weaver, V.M., Petersen, O.W., Larabell, C.A., Dedhar, S., Briand, P., Lupu, R. and Bissell, M.J. (2002) Phenotypic reversion or death of cancer cells by altering signaling pathways in three-dimensional contexts

Reciprocal interactions between beta1-integrin and epidermal growth factor receptor in three-dimensional basement membrane breast cultures: a different perspective in epithelial biology. *J Natl Cancer Inst*, **94**, 1494-1503.

Weaver, V.M., Lelievre, S., Lakins, J.N., Chrenek, M.A., Jones, J.C., Giancotti, F., Werb, Z. and Bissell, M.J. (2002) beta4 integrin-dependent formation of polarized three-dimensional architecture confers resistance to apoptosis in normal and malignant mammary epithelium. *Cancer Cell*, **2**, 205-216.

Weaver, V.M., Petersen, O.W., Wang, F., Larabell, C.A., Briand, P., Damsky, C. and Bissell, M.J. (1997) Reversion of the malignant phenotype of human breast cells in three-dimensional culture and in vivo by integrin blocking antibodies. *J Cell Biol*, **137**, 231-245.

Zardi, L., Carnemolla, B., Siri, A., Petersen, T.E., Paolella, G., Sebastio, G. and Baralle, F.E. (1987) Transformed human cells produce a new fibronectin isoform by preferential alternative splicing of a previously unobserved exon. *Embo J*, **6**, 2337-2342.

Figure legends

Figure 1. Restoration of mammary cell polarization and morphogenesis from tumorigenic to normal by experimentally manipulation in the context of ECM.

Zeiss LSM 510 laser Scanning confocal images revealing the morphology and polarization of MCF10A acini (**A-C**), transformed tumorigenic T4-2 aggregates (**D-F**) and reverted T4-2 acinus like structures (**G-I**) in 3D culture. **A, D, G** represent Differential Interference Contrast (DIC) micrograph of two-week old cultures on Matrigel fixed and immune stained as described in materials and methods. **B, E** and **H** show localization of β4-integrin revealed by immune-staining and fluorescent laser Scanning confocal. **C, F** and **I** represent the distribution of beta catenin revealed by immune staining. Alexa 546-immune-labeled proteins (β4-integrin or β-catenin) are seen as red fluoresecent and blue fluorescent represent nuclei stained with DAPI. Reversion of T4-2 was obtained with a combination of PI3K-inhibitor LY290042 and dibutyryl-cAMP as described in materials and methods.

Figure 2. Differential DNA digestion of chromatin harbored in normal versus tumorigenic mammary epithelial cells grown in 2- and 3- D cell cultures.

Fluorescent micrograph of nonmalignant (MCF10A) and tumorigenic (T4-2) mammary epithelial lines. The dry monolayer smears of each culture was incubated without (**A** and **C**) or with Alu I (**B** and **D**) for 1.5 h at 37˚C and stained with EtBr, to analyze the digested DNA by fluorescent microscopy. **E-H** represents flow cytometry comparing the DNA profile of nonmalignant MCF10A and tumorigenic T4-2 cells before (**E** and **G**) and after (**F** and **H**) 60 min of Alu I digestion respectively. DNA profile was determined by fluorescent intensity of propidium iodide and was used as a measure of DNA digestion. The gating for M1 and M2 indicates nucleus off cell cycle (digested) and in cell cycle (undigested). **J** and **K** represent fluorescent high magnification micrographs visualizing the amount DNA digestion in nonmalignant MCF10A and tumorigenic T4-2 nuclei treated similar to samples applied in flow cytometry. A Graphical illustration of flow cytometry analysis measurements of nonmalignant (MCF10A) and tumorigenic (T4-2) chromatin digestion is shown in panel I. Percent DNA digestion is determined by relative increase of fluorescent intensity gated in M1 before and after digestion. Error bars indicate the standard error over mean from 5 separate identical experiments. Laser Scanning confocal images comparing chromatin of undigested DNA in nonmalignant MCF10A

(**L, P**) and tumorigenic T4-2 (**M, Q**) cells cultured for two weeks on Matrigel, permeabilized and stained as described in Materials and Methods. Bright field images of 3-D cultures treated as described above followed by Trypan blue staining, was included to illustrate complete permeabilization of MCF10A acini (**R**), reverted T4-2 acinus-like structures (**S**) and transformed T4-2 aggregates (**T**). Laser Scanning confocal images comparing chromatin of Alu I digested DNA in nonmalignant MCF10A acini (**U, Y**) and transformed T4-2 aggregates (**V, Z**). Cultures were permeabilized as described above before Alu I treatment (**W, X**) and nuclei were stained with EtBr and DAPI and observed by fluorescence laser imaging. Note the complete digested nuclei revealed by higher magnification micrographs of normal spheroids in contrast to the almost undigested nuclei in tumorigenic aggregates.

Figure 3. Reversible manipulation of phenotype and genome sequestration

Laser Scanning confocal images comparing DNA digested chromatin in transformed T4-2 aggregates (**A,C,F,G**) and reverted T4-2 acinus-like structures (**B,D,E,H**). Cells were grown for two weeks on Matrigel without (**A,C,F,G**) and with 6 μM LY294002 and 1mM dibutyryl-cAMP (**B,D,E,H**), followed by permeabilization and AluI digestion for 24h as described in materials and methods. Digested nuclei were stained with EtBr and observed by fluorescence laser imaging (B,D) and bright-field images were obtained by DIC (**C,D,G,H**). Note in the higher magnification images that only the nucleolus remains undigested in the nuclei of completely digested T4-2 revertants (**E**), in contrast to only partially digested chromatin in transformed T4-2 (**F**). These data are representative images of observations obtained from 5 separate identical experiments. **I-K** are phase contrast images of revertant T4-2 acinus-like structures treated for two weeks with 6 μM LY294002 and 1mM dibutyryl-cAMP and then released from drug at day 0 (**I**), day 7 (**J**) and day 15 (**K**) after drug release. **L-Q** are Laser scanning confocal images of T4-2 cultures treated similar to **I-K**, followed by permeabilization and 24h AluI incubation. Fluorescent micrographs (based on EtBr stained DNA) reveal DNA digestion by Alu I at day 0 (**L**), day 7 (**M**) and day 15 (**N**) after drug release. Note the gradual shift from normal to tumorigenic morphology accompanied by a similar shift in AluI sensitivity. **O, P, Q** are bright-field image obtained by DIC corresponding to **L, M, N**. These data are representative for 3 separate identical experiments. The percentage of digested DNA before and after Alu I digestion on revertant T4-2 at day 0, day 7 and day15 after drug release (similar to above) is listed in panel R. Quantitation of digested DNA was

performed by Flow cytometry analysis and measured as signal-intensity gated in M1 see Materials and Methods. Numbers represent the mean of 3 separate identical experiments.

Figure 4. cAMP-induced reversion of morphology, polarization and chromatin organization involves a PKA coupled signal

A-D are phase contrast micrographs comparing the morphology of T4-2 cells grown for 14 days on Matrigel in the presence (A,B,G) or absense (H) of different cAMP analogs; N6-monobutyryl-cAMP (**A**), dibutyryl-cAMP + LY294002 (**B**), 8-CPT-2-O´-Me-cAMP (**G**) or untreated (**H**). Laser scanning images revealing the β4-integrin localization in T4-2 cultures treated for two weeks with either N6-monobutyryl-cAMP (**D**) or no drug (**J**) followed by immune staining as described in Materials and Methods. Red indicates β4-integrin and blue show DAPI stained nuclei. Corresponding bright field images to **D** and **J** are shown by DIC in (**C** and **I** respectively). Laser scanning images revealing nuclei of T4-2 cultures treated for two weeks with either monobutyryl-cAMP (**F**) or no drug (**L**) followed by permeabilization, 24h AluI digestion and EtBr staining as previously described. Corresponding bright field images to F and L are show by DIC in (**E** and **K** respectively). These data are representative for three separate identical experiments.

Figure 5. Reversion of morphology, polarization and chromatin organization by interfering with the communication of ECM components.

Phase contrast micrographs comparing the morphology of T4-2 cells grown for 14 days on Matrigel in the presence of different antibodies; treatment with anti- fibronectin (anti-FN, **A**), anti-collagen I (anti-COL I, **B**), anti-collagen IV (anti-COL IV, **C**), anti-laminin (anti-LAM, **D**), non specific IgG (IgG, **E**). All images (**A-E**) are at 200 X magnifications.

Laser scanning confocal images of T4-2 cells grown and treated as described in **A-E**, followed by immune staining with anti- β4-integrin (shown in red) to reveal structural polarization in anti-fibronectin treated cultures (**G**), anti collagen I treated cultures (**H**), anti laminin trated cultures (panel I) and IgG treated cultures (**J**). T4-2 cells treated with combination of 6 μM LY294002 and 1mM dibutyryl-cAMP (cAMP cocktail, **F**) represents a polarized control and untreated cultures (Untreated, **K**) represent an unpolarized control. Blue represent DAPI stained nucleus (se Materials and Methods). Corresponding fields to fluorescent images in **F-K** are represented in bright field (obtained by DIC) in **F´-K´** respectively. **L-W** are Laser scanning images of T4-2 cells

grown and treated as above followed by permeabilization, 24h AluI digestion and EtBr staining (see Materials and Methods). Alu I digested T4-2 aggregates (untreated, **L**, **M**) and reverted T4-2 (cAMP-cocktail, panel **N,O**) represent controls for AluI resistant and sensitive chromatin respectively. Both low and high magnification images are shown of AluI digested T4-2 cultures treated with anti-fibronectin (anti-FN, **P-S**) and anti-laminin (anti-LAM, **T-W**). Corresponding DIC images are shown to the left of each fluorescent micrograph (**M, O, Q, S, U, W**).

Table 1.

T4-2 cultures[1]	Morphology	Polarization[2]	DNA digestion[3]
Untreated	Disorganized aggregate	-	Resistant
LY249002/dibutyryl-cAMP	Acinus-like	+	Sensitive
Anti fibronectin	Acinus-like	+	Sensitive
Anti collagen I	Spheroid	-	ND
Anti collagen IV	Spheroid	ND	ND
Anti laminin	Horizontal plague	-	Resistant
Anti IgG	Disorganized aggregate	-	Resistant

[1] Cultures of T4-2 cells grown in 3-dimmension for 14 days in the presences of different agents (as indicated) before analyzed.

[2] Determined by β4-integrin distribution (revealed by immune staining) and hollow lumen (revealed by nucleus orientation). See Materials and Methods.

[3] The sensitivity of DNA was determined by 24h Alu-I digestion (Materials and Methods)

Figure 1

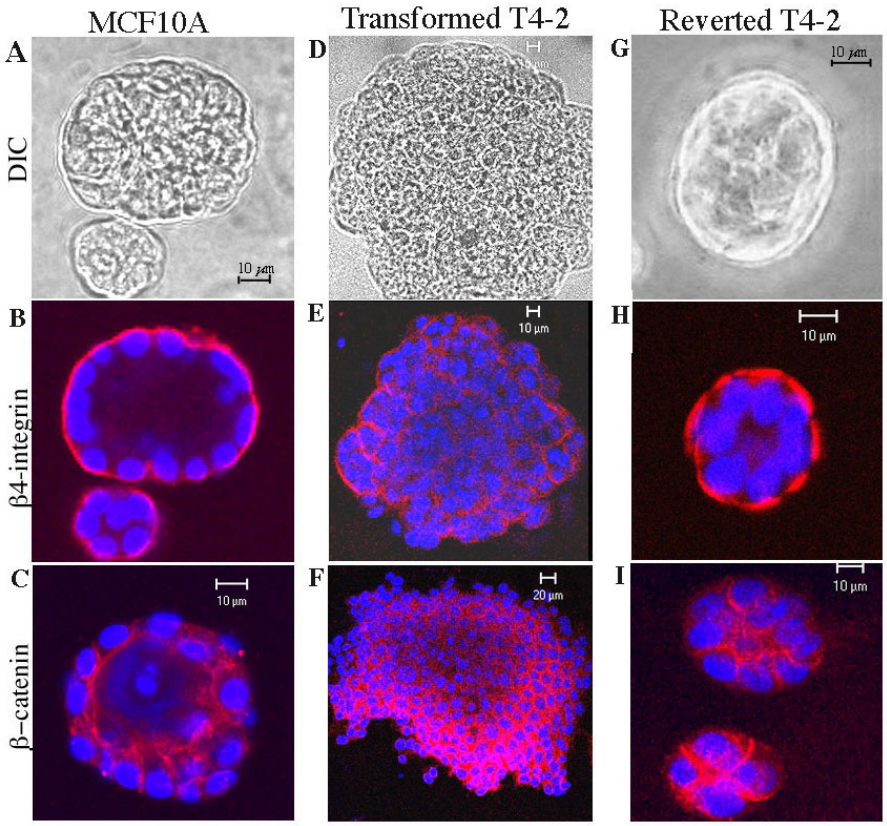
MCF10A
Transformed T4-2
Reverted T4-2
A
D
G
DIC
10 μm
B
E
H
β4-integrin
10 μm
C
F
I
β−catenin
10 μm
20 μm
10 μm

Figure 2

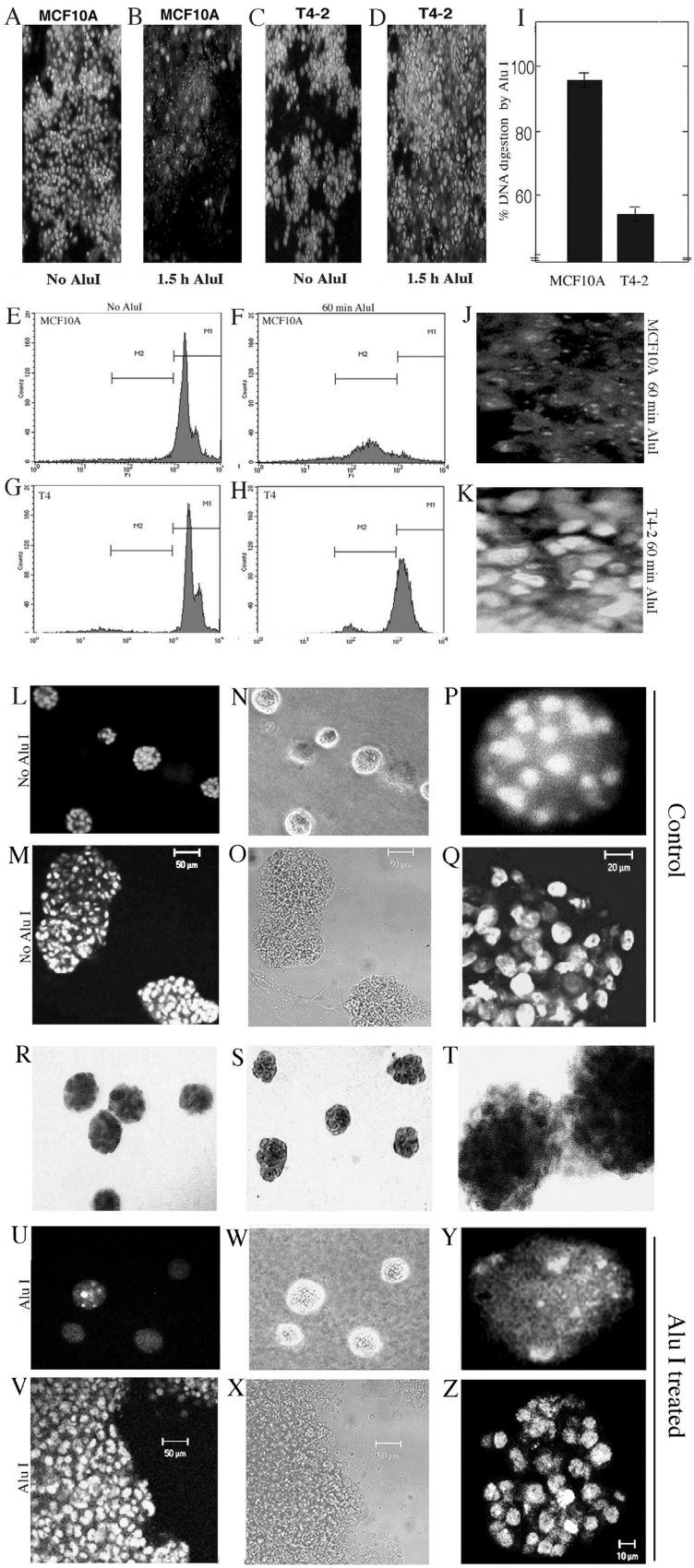
A MCF10A
B MCF10A
C T4-2
D T4-2
No AluI
1.5 h AluI
No AluI
1.5 h AluI
I
% DNA digestion by Alu I
100
80
60
MCF10A
T4-2
E
No AluI
MCF10A
M1
M2
F
60 min AluI
MCF10A
M1
M2
J
MCF10A 60 min AluI
G
T4
M1
M2
H
T4
M1
M2
K
T4-2 60 min AluI
L
No Alu I
N
P
M
No Alu I
50 µm
O
50 µm
Q
20 µm
Control
R
S
T
U
Alu I
W
Y
V
Alu I
50 µm
X
50 µm
Z
10 µm
Alu I treated

Figure 3

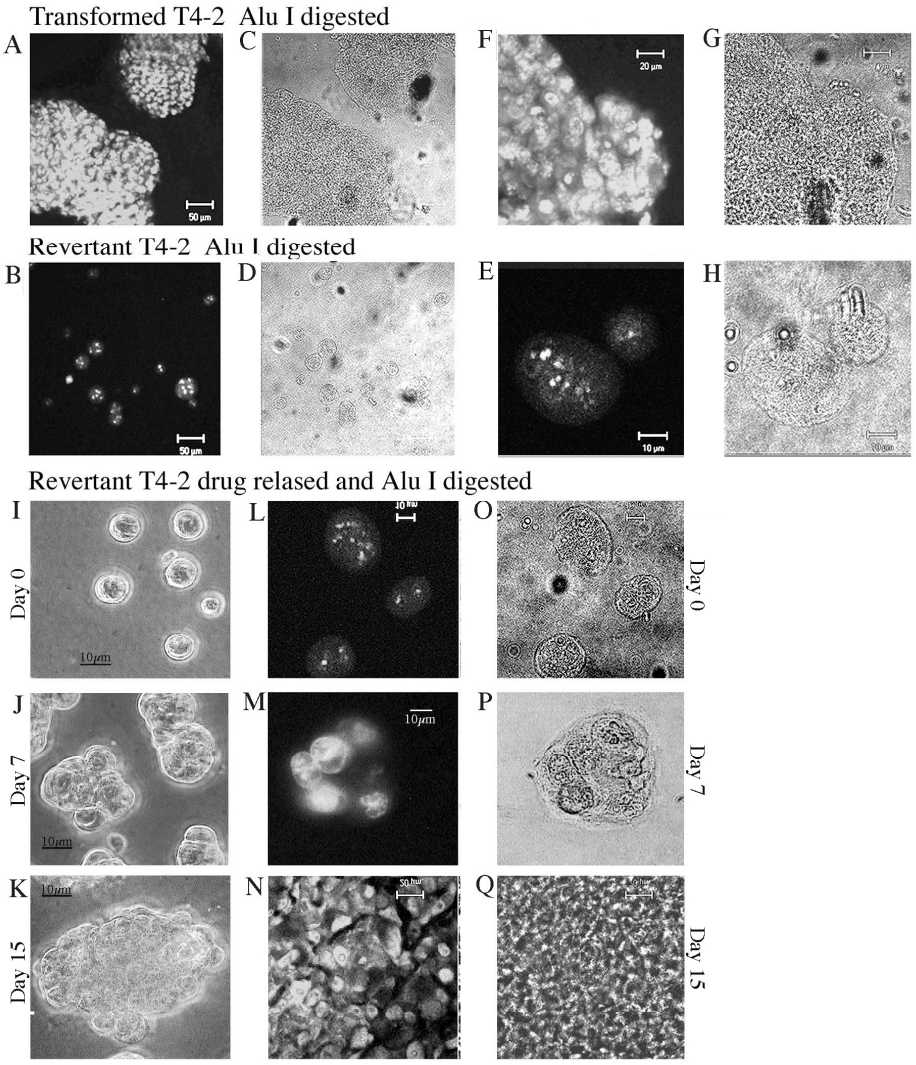

R

% DNA	No Alu M1	24h AluI M1
T4 reverted-released 0 days	3%	71.5%
T4 reverted-released 7 days	4.8%	10%
T4 reverted-released 15 days	4.1%	5%

Figure 4

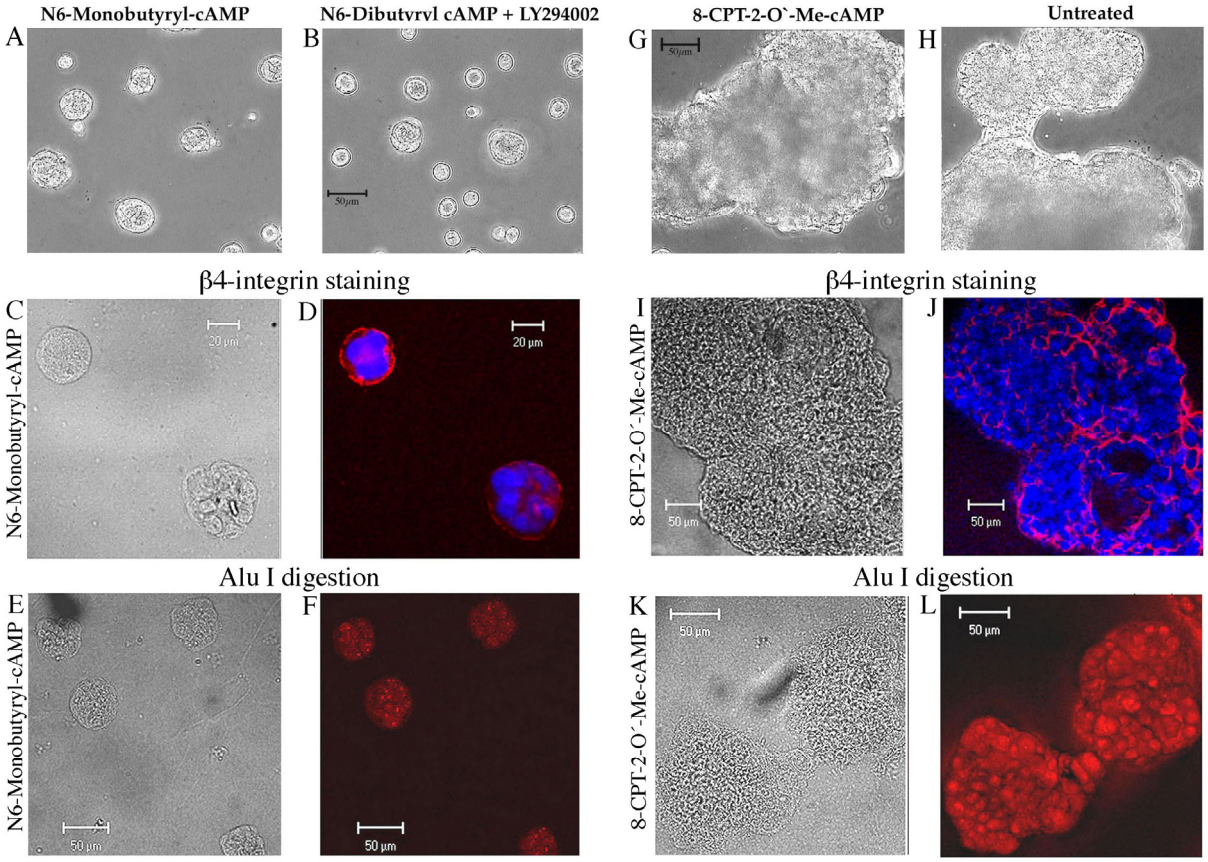
N6-Monobutyryl-cAMP
N6-Dibutvrvl cAMP + LY294002
8-CPT-2-O`-Me-cAMP
Untreated
A
B
G
H
β4-integrin staining
β4-integrin staining
C
D
I
J
N6-Monobutyryl-cAMP
8-CPT-2-O´-Me-cAMP
20 µm
20 µm
50 µm
50 µm
Alu I digestion
Alu I digestion
E
F
K
L
N6-Monobutyryl-cAMP
8-CPT-2-O´-Me-cAMP
50 µm
50 µm
50 µm
50 µm

Figure 5

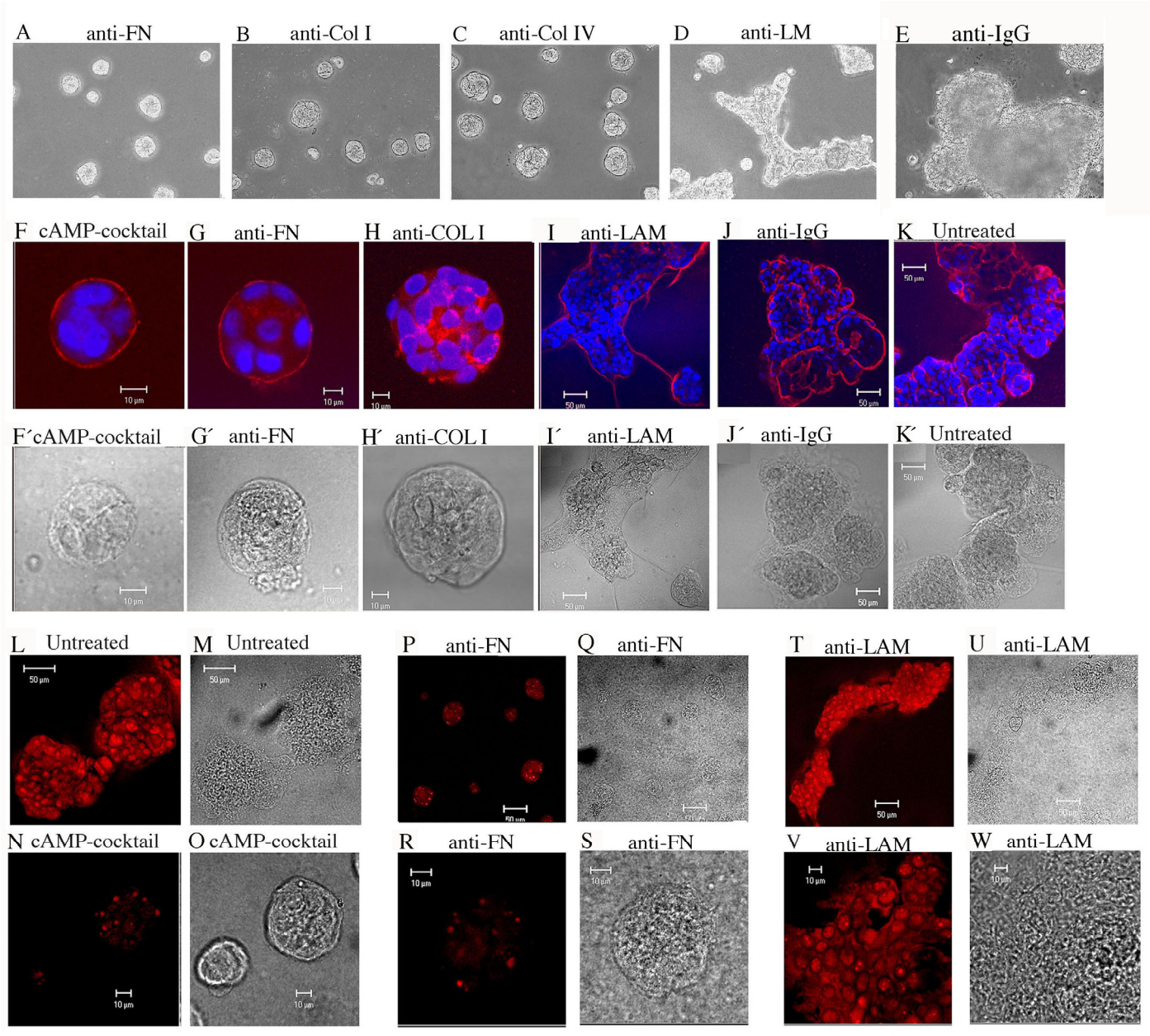
A anti-FN
B anti-Col I
C anti-Col IV
D anti-LM
E anti-IgG
F cAMP-cocktail
G anti-FN
H anti-COL I
I anti-LAM
J anti-IgG
K Untreated
F´cAMP-cocktail
G´ anti-FN
H´ anti-COL I
I´ anti-LAM
J´ anti-IgG
K´ Untreated
L Untreated
M Untreated
P anti-FN
Q anti-FN
T anti-LAM
U anti-LAM
N cAMP-cocktail
O cAMP-cocktail
R anti-FN
S anti-FN
V anti-LAM
W anti-LAM